Proceedings of the 9ICEG
9th International Congress on Environmental Geotechnics
25-28 June, 2023 | Chania, Greece

https://doi.org/10.53243/ICEG2023-114

Infiltration study on compacted clay liners subjected to wet-dry cycles

A. S. Devapriya[1], and T. Thyagaraj[2]

[1]*Research scholar, Indian Institute of Technology Madras, Chennai, India, email: devapriya.as09@gmail.com*

[2]*Professor, Indian Institute of Technology Madras, Chennai, India, email: ttraj@iitm.ac.in*

ABSTRACT

Compacted clay barriers used as liners and covers in landfills are subjected to alternate wet-dry cycles. During the drying cycles, the compacted clay loses the moisture content, which results in shrinkage and the formation of desiccation cracks in them. These desiccation cracks act as preferential flow paths, through which fluids percolate and reduce the efficiency of the clay barrier. The cracks formed during the drying cycle may heal during the subsequent wetting cycles when the clay absorbs moisture and swells. However, the swelling process is not instantaneous, and the healing of the cracks takes time, during which the leachate can infiltrate into the underlying ground. The healing capacity of the clay may also be hampered as the soil is subjected to repeated cycles of wetting and drying. Hence, in addition to studying the hydraulic conductivity of the compacted clays, infiltration studies must be carried out on compacted clay to understand its hydraulic behaviour. The present study is conducted on a compacted red soil-bentonite mixture to understand the effect of wet-dry cycles on its infiltration behaviour. The tests were carried out using an in-house fabricated oedometric-infiltrometer test apparatus, using distilled water as the percolating fluid. The inflow and the outflow of DW through the specimens were measured at specific time intervals until the inflow and outflow reached equilibrium. The study showed a variation in the flow patterns through the soil specimens with the increase in the wet-dry cycles, indicating that the wet-dry cycles influence the infiltration behaviour of the compacted soil.

Keywords: Compacted clay liners, wet-dry cycle, infiltration, hydraulic conductivity

1 INTRODUCTION

Clay liners are an integral part of both hazardous and municipal landfills. The liners act as a physical barrier between the waste deposit and the surrounding environment. Liners provided at the top, called covers or caps, isolate the waste from the atmosphere and prevent the seepage of water into the underlying waste. The liners at the bottom separate the waste from the soil and groundwater and prevent the leachate from coming into contact with them (Cossu and Stegmann, 2018a). Hence, for a landfill liner to be effective, it should have a very low hydraulic conductivity. Various Environment Protection Agencies (EPAs) require the hydraulic conductivity of the compacted soil liners to be less than or equal to 1×10^{-7} cm/s. In addition to the saturated hydraulic conductivity, another significant parameter is the infiltration into the soil. McBrayer *et al.* (1997) defined infiltration as the downward entry of water into the soil. The desiccation cracks are formed during drying, which gets closed during the subsequent wetting phase. However, the closing of cracks is not instantaneous, and large flow occurs through the cracks, which becomes the preferential flow path. Hence the measurement of hydraulic conductivity alone, while the soil is fully saturated, can underestimate the efficiency of the compacted clay to contain the leachate, and therefore infiltration studies are of great importance in the field.

Infiltration tests were conducted by McBrayer *et al.* (1997) on compacted kaolin samples and discovered that the flow occurs in two stages, an initial dynamic stage, which occurs before the cracks get closed and later, a steady-state stage, which occurs after the cracks are healed. They also found that the cracks do not fully heal even after the end of the wetting cycle. However, Day (1998) conducted infiltration tests on montmorillonite specimens and found that the cracks completely healed after the wetting cycle. He concluded that the healing of cracks depends on the type of clay mineral present in the soil. Infiltration studies on compacted specimens subjected to wet-dry cycles show that the desiccation cracks in the soil act as preferential flow paths, resulting in large infiltration flow in the specimen (Li *et al.,* 2016).

Cheng *et al.* (2021) conducted infiltration tests on compacted clay specimens to study the infiltration through the cracks formed due to alternate wet-dry cycles. They observed the soil cracking after the second drying cycle, and for those samples, the infiltration occurred in three different stages: an initial rapid stage of infiltration, a second stage where the infiltration decreases dramatically, and then finally slows down to reach the final equilibrium stage. They defined the time between the first and second stages to be the prehealing time of cracks. Similar stages of flow were found in compacted expansive soil by Julina and Thyagaraj (2021), where they carried out infiltration tests on compacted expansive soil using an in-house fabricated test set-up.

Most of the studies focused on the hydraulic conductivity of the saturated compacted soils, and infiltration studies on compacted soils subjected to alternate wet-dry cycles are lacking. This paper hence presents the infiltration behaviour of a compacted red soil-bentonite mixture when subjected to alternate wet-dry cycles. The tests were carried out in an oedometric-infiltrometer test apparatus-fabricated in-house (Julina and Thyagaraj, 2021)-that allows simultaneous measurement of the inflow infiltration rate, outflow infiltration rate, percentage swell, and hydraulic conductivity of the soil specimen.

2 MATERIALS AND METHODS

The experimental studies were conducted on an Indian red soil modified with 10% bentonite by weight. The red soil was taken from IIT Madras, Chennai, India. The soil was first sieved through the 2 mm sieve, air-dried, pulverized, and then mixed with a commercially available bentonite to obtain the red soil-bentonite mixture R90-B10. The basic properties of red soil, bentonite and R90-B10 are presented in Table 1.

The infiltration tests were carried out on an R90-B10 specimen in its as-compacted state and in the desiccated state after different drying cycles (see Figures 1.a and 1.c).The tests were performed using an in-house fabricated oedometer-infiltration test set-up (Julina and Thyagaraj, 2021). The infiltration test set-up consists of an oedometric-infiltrometer cell, oedometer frame, Marriott tube to maintain a constant head, inflow, and outflow arrangements (see Figure 2).

For preparing the specimen, the red soil-bentonite mixture R90-B10 was first prewetted with distilled water (DW) amounting to its optimum moisture content (OMC). After checking for its water content, the prewetted soil was compacted into an oedometer ring of diameter 75 mm and height 50 mm to a height of 20 mm, such that its dry unit weight was attained. A filter paper was placed on the top, and a dry porous stone was placed in the ring. The oedometer ring was then placed in the oedometer cell, on the top of a slotted acrylic disc. The oedometer cell was then placed on the oedometer frame. A loading cap connected with inflow tubes, which are connected to the Marriott tube, was placed over the specimen. The Marriott tube was filled with DW, which was used to study the infiltration tests for the present study. The flow from the Marriott tube into the specimen through the inflow pipes was controlled using valves. The Marriot tube was placed over a weighing balance, and the weight was noted at different time intervals during the test to measure the inflow into the specimen. The DW flowing out through the specimen was collected in a beaker whose weight was also continuously noted to measure the outflow infiltration.

Table 1. *Properties of red soil, bentonite and R90-B10 red soil-bentonite mixture (After Devapriya and Thyagaraj, 2021)*

Property	Red soil	Bentonite	R90-B10
Liquid limit (%)	34	224	86
Plastic limit (%)	20	48	27
Shrinkage limit (%)	15	8.4	15
Plasticity index (%)	14	176	59
Specific gravity, G_s	2.68	2.92	2.70
Grain size distribution (%)			
Sand	66	0	60
Silt	15	29	16
Clay	19	71	24
Unified Soil Classification Symbol (USCS)	SC	CH	SC
Maximum dry unit weight (kN/m^3)	19.4	-	18.75

Optimum moisture content, OMC (%)	11	-	12.5
Unconfined compressive strength (kPa)	212	-	230
Hydraulic conductivity (cm/s)	1.98×10^{-5}	-	2.69×10^{-8}

The tests were conducted in two stages: (i) stage I and (ii) stage II of testing. During stage I, the set-up was arranged such that the flow occurs at a hydraulic gradient of 2. Stage I is continued till the inflow and the outflow attains a constant value. The hydraulic gradient of 2 was adopted to simulate the hydraulic gradient in the natural soil system, which ranges from 1 to 5 (Ranjan and Karthigesu, 1996; Julina and Thyagaraj, 2021). The inflow and outflow volumes of the DW were measured by noting the change in the weighing balance readings. The Stage I readings were noted until the flow through the specimen reached a steady state, wherein the inflow and the outflow volumes attain a constant value. The vertical swell was also measured during this stage by noting the dial gauge readings at regular intervals. At the stage II of the testing, the test set-up was repositioned such that the flow through the specimens occurs at a hydraulic gradient of 20, so as to measure the hydraulic conductivity as per the ASTM requirements (ASTM D5084-16a 2016).

The incremental inflow and outflow infiltration rates were calculated using equation 1.

$$I_{inflow} \text{ or } I_{outflow}\ (\text{cm/s}) = Q/At \quad (1)$$

Where Q is the inflow or outflow volume (cm^3), A is the cross-sectional area of the oedometric ring (cm^2), and t is the time taken for the inflow or outflow (s).

The hydraulic conductivity was calculated using equation 2.

$$k\ (\text{cm/s}) = \text{Steady state } I_{inflow} \text{ or } I_{outflow} / \text{ Hydraulic gradient} \quad (2)$$

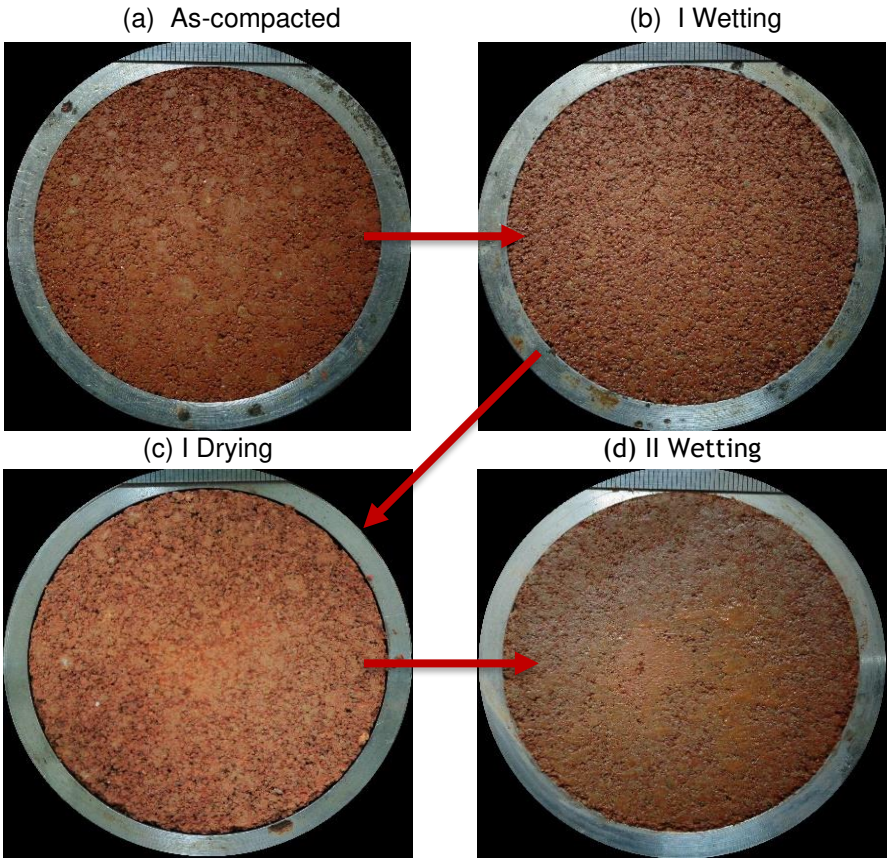

Figure 1. *Digital camera images of bottom surfaces of compacted red soil-bentonite specimens at the end of different stages of wet-dry cycles*

After the completion of the infiltration tests on the R90-B10 specimen in its as-compacted state, (i.e., after 1st wetting cycle), the specimen was oven-dried at a constant temperature of 45±2°C until there was no further change in the water content in the soil. The temperature in the oven was maintained at 45±2°C to accelerate the drying and to simulate adverse field conditions in the specimens (Thyagaraj and Zodinsanga, 2014). After the complete drying of the specimen, which took about 5 days, the next infiltration test was carried out on the desiccated specimen, following the same procedure as explained in the paragraphs above. The tests were repeated for five wetting and drying cycles, at the end of which the volumetric deformations during the swell-shrink cycles became constant and the specimen reached equilibrium (Devapriya and Thyagaraj, 2021). Further, the tests were repeated on an additional identical specimen to confirm the repeatability of the tests. The results obtained on the as-compacted specimen and the desiccated specimens after 1st, 2nd and 4th drying cycles are presented and discussed in the subsequent section.

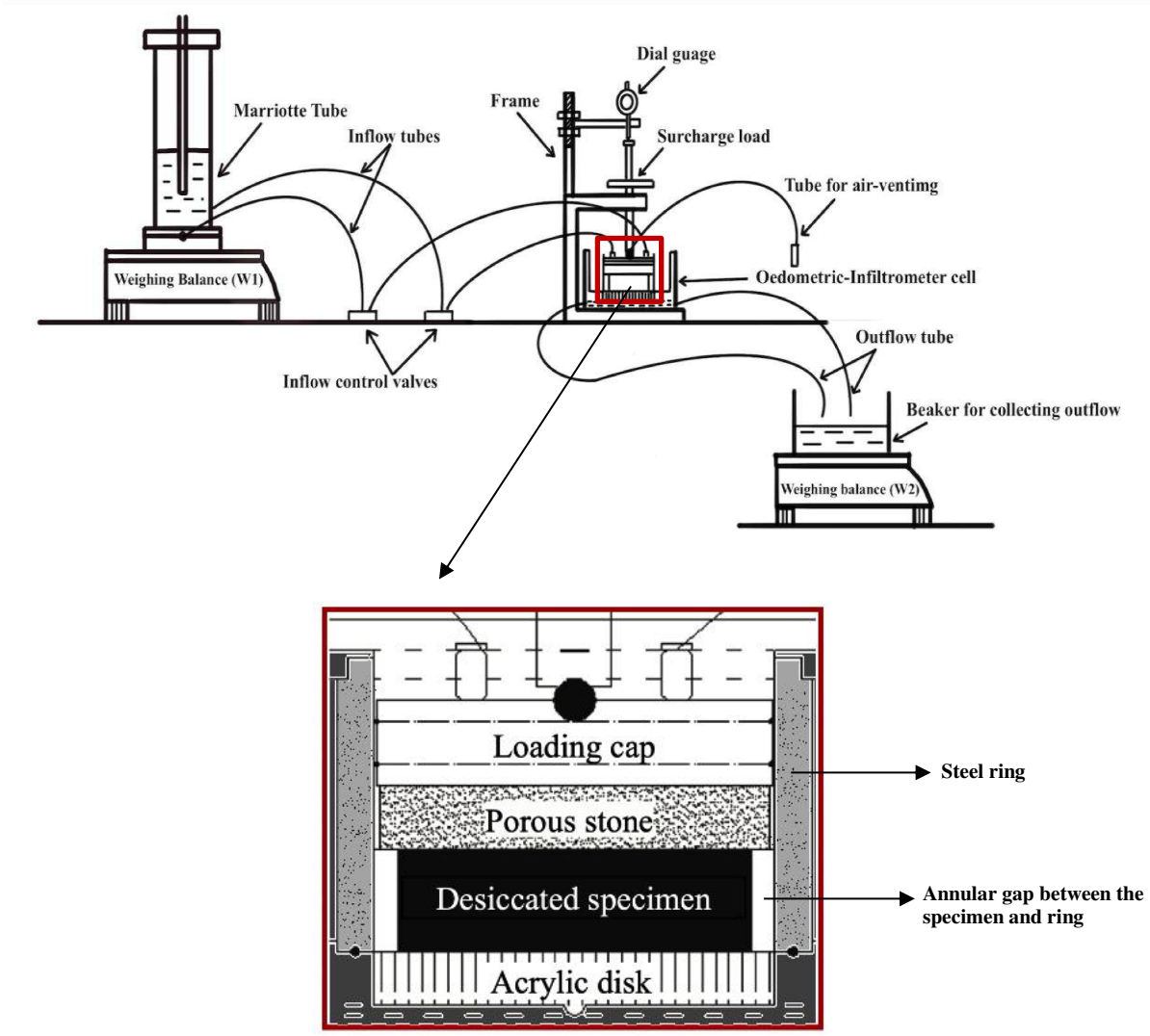

Figure 2. *Schematic diagram of oedometric-infiltrometer test set-up (after Julina and Thyagaraj, 2021)*

3 RESULTS AND DISCUSSION

3.1 Infiltration behaviour

Figures 3-6 present the inflow infiltration rate (I_{inflow}), outflow infiltration rate ($I_{outflow}$), hydraulic conductivity and percentage swell with time of compacted R90-B10 specimen in the as-compacted state and after

1st,2nd and 4th drying cycles, respectively. The infiltration plots of the desiccated specimens (see Figures 4-6) can be divided into three distinct regions: i) Initial outflow region, ii) No outflow region and iii) Permeation outflow region (see Figure 4; Julina and Thyagaraj 2021). The initial outflow region is marked by high infiltration and outflow. In this zone, the flow happens mainly through the annular gap between the desiccated specimen and the oedometer ring, which formed when the soil specimen shrunk laterally (see Figure 1.c). An annular gap is a technical crack, and a large amount of flow occurs through it before it closes. Large flow can also occur through any desiccation microcracks that might have formed due to shrinkage during the drying cycle. The compacted soil in its desiccated state is characterized by large matric suction, which gets dissipated by the absorption of DW. As the soil absorbs water, the soil undergoes swelling. The swelling in the lateral direction happens in unrestrained condition, while the load on the specimen restricts the vertical swell. As the specimens swell laterally the annular gap closes, thus sealing the space between the specimen and the ring. At this point the outflow reduces and becomes zero, marking the beginning of the no outflow zone. The no outflow zone is also marked by primary swelling, where the soil specimen swells rapidly in the vertical direction. The soil becomes almost completely saturated, filling all the macropores in the specimen, and after a while, the outflow restarts, thus marking the beginning of the permeation outflow region. In the permeation outflow region, the inflow and outflow eventually become equal, implying that the specimen has reached a steady state (Julina and Thyagaraj, 2021).

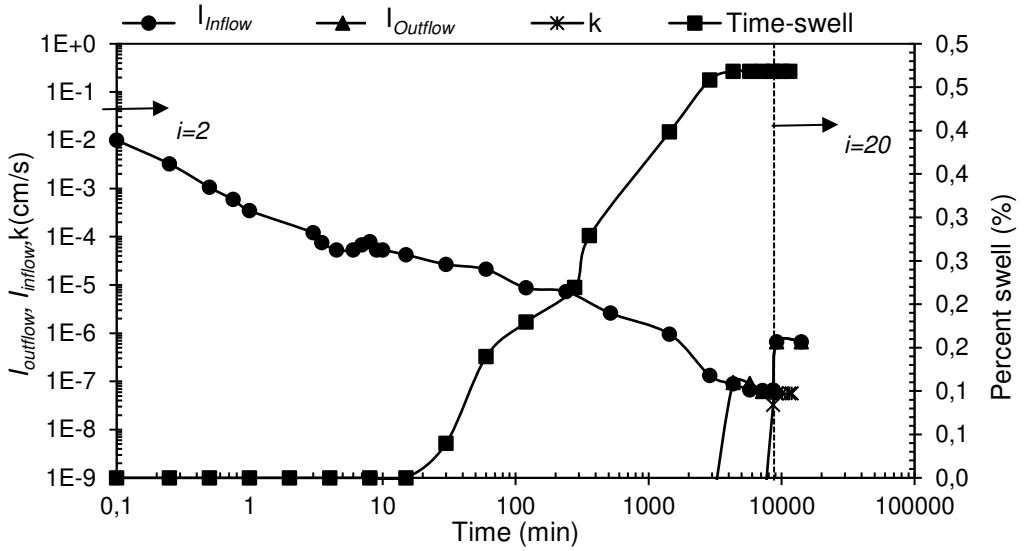

Figure 3. *Variation of I_{inflow}, $I_{outflow}$, hydraulic conductivity and percentage swell with time of R90-B10 in the as-compacted state*

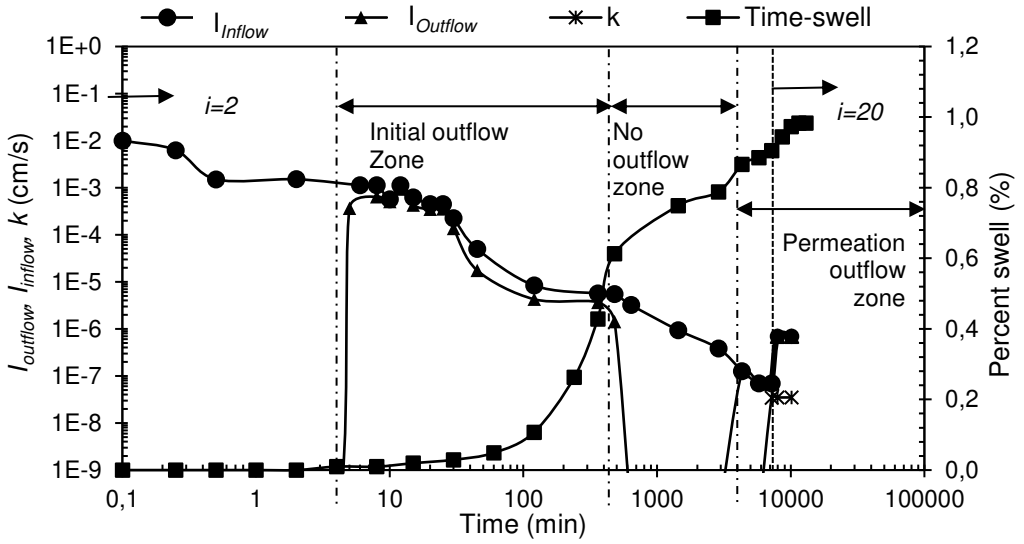

Figure 4. *Variation of I_{inflow}, $I_{outflow}$, hydraulic conductivity and percentage swell with time of R90-B10 after 1st drying cycle*

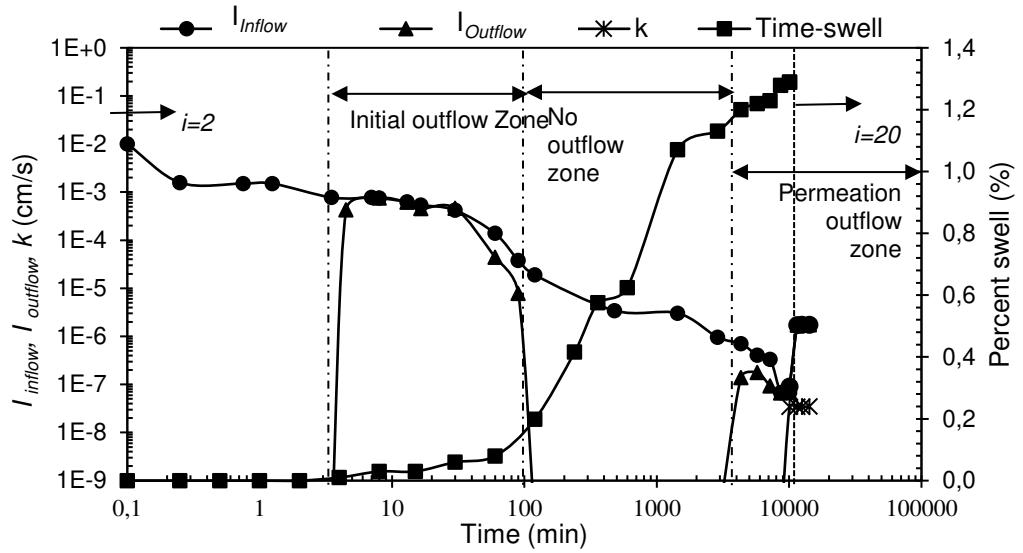

Figure 5. *Variation of I_{inflow}, $I_{outflow}$, hydraulic conductivity and percentage swell with time of R90-B10 after 2nd drying cycle*

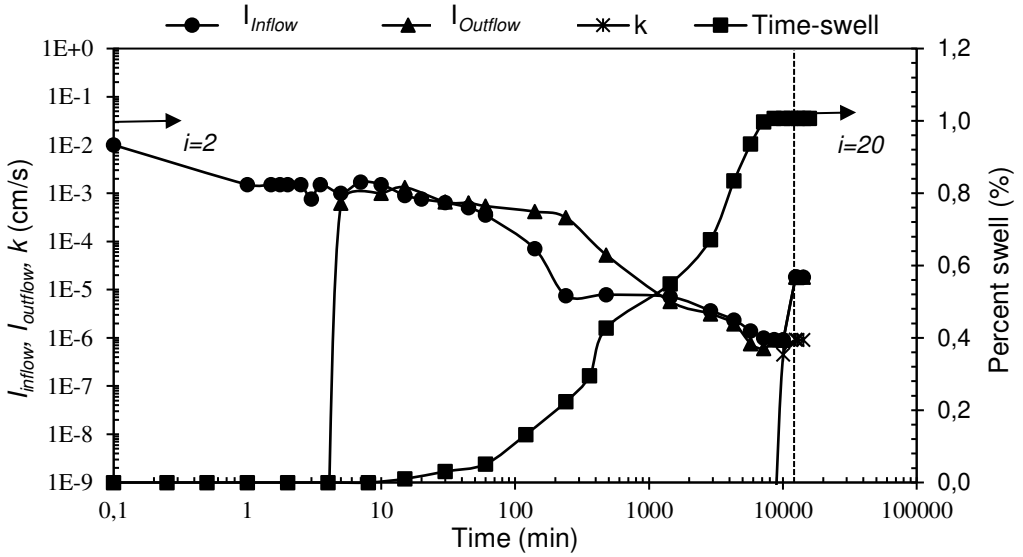

Figure 6. *Variation of I_{inflow}, $I_{outflow}$, hydraulic conductivity and percentage swell with time of R90-B10 after 4th drying cycle*

There is no initial outflow zone for the R90-B10 specimen in the as-compacted state (see Figure 3) due to the absence of the annular gap between the ring and the specimen (see Figure 1.a). The infiltration rate is also lower compared to the desiccated soil specimens due to the higher water content in the specimen. After 1st drying, as the specimen shrunk vertically and laterally, the annular gap formed between the ring and the specimen (see Figure 1.c and 2), and initial outflow zone was recorded in the specimen. The initial outflow commences 4-5 mins from the beginning of the inflow through the specimen. The initial outflow continued until 480 mins, when the annular gap gets completely closed (see Figures 1.d and 4). During the 3rd infiltration cycle, the time required to complete the initial outflow zone was observed to be lesser when compared to the other desiccated specimens. The specimen during this cycle also showed the highest swell potential compared to the other wetting cycles. The higher swell resulted in the quicker closure of the annular gap, resulting in a shorter initial outflow zone. The permeation outflow during the first three infiltration cycles began at 4320 minutes, once the specimen reached saturation, and eventually reached a steady state. The 5th infiltration cycle on the desiccated specimen (after the 4th drying cycle) showed a significant difference in the infiltration behaviour of the soil. It can be observed from Figure 6 that the no-outflow zone is absent during this cycle. The absence of the no-outflow zone indicates that the water retaining capacity of R90-B10 reduced with the wet-dry cycles. During the drying cycle, micro desiccation cracks were formed in the

compacted soil, which becomes the preferential path for the water flow in the compacted specimens. Even though these cracks heal during the next wetting cycle, as the soil is subjected to alternate wetting-drying cycle, the swelling is reduced, and the healing capacity of the soil deteriorates. Hence, the microcracks remained unhealed during the wetting cycle, and the infiltration occurred continuously through the specimen.

3.2 Hydraulic conductivity

After the completion of stage I of testing, when the steady state flow was attained in the permeation outflow zone, the stage II of testing was commenced, where the test-set up was repositioned, and the flow occurred at a hydraulic gradient of 20. The hydraulic conductivity was calculated using equation 2. Figure 7 compares the hydraulic conductivity measured during stage II of each wetting cycle. Figure shows that the hydraulic conductivity increased with alternate wet-dry cycles, indicating that the microcracks formed does in fact as the preferential flow paths. However, until the 3rd cycle, the hydraulic conductivity is lower than the hydraulic conductivity criterion of 1×10^{-7} cm/s, whereas the value is much higher at the end of the 5th wetting cycle, which confirms that the healing ability of the R90-B10 specimen has deteriorated with the alternate wetting and drying.

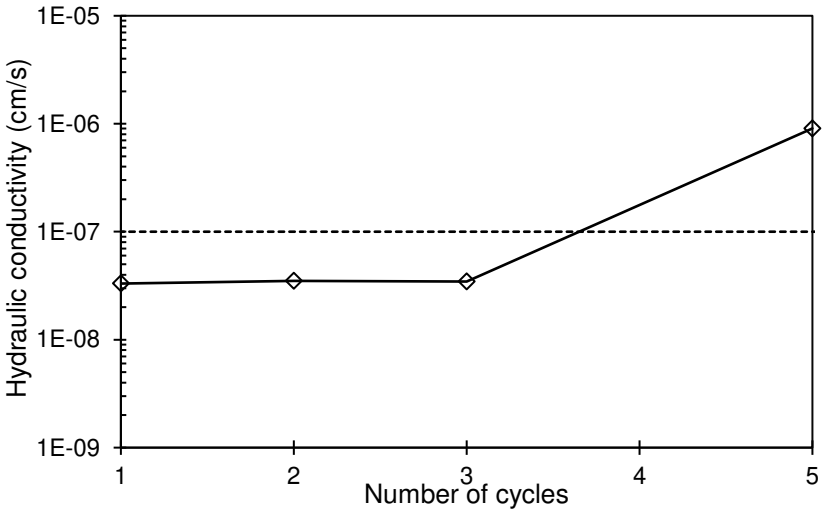

Figure 7. *Variation of hydraulic conductivity of R90-B10 specimens with wet-dry cycles*

4 CONCLUSIONS

The laboratory infiltration studies conducted on compacted red soil-bentonite mixture showed that the alternate wet-dry cycle affects the healing capacity of the soil. The infiltration plots of the compacted specimen can be divided into three different regions: the initial inflow zone, the no outflow zone, and the permeation outflow zone. The infiltration behaviour of the desiccated soil specimens was directly linked to their swelling behaviour. The inability of the soil to swell and heal the desiccation cracks resulted in the elimination of the no-outflow zone in the compacted R90-B10 red soil-bentonite mixture, resulting in the continuous flow of the permeant through it. Thus, the wet-dry cycles affect the efficiency of the R90-B10 red soil-bentonite mixture to hold the permeants, thus indicating that the mixture needs more bentonite to preserve its swelling ability during the wet-dry cycles.

REFERENCES

ASTM D5084-16a. (2016). Standard test methods for measurement of hydraulic conductivity of saturated porous materials using a flexible wall permeameter. West Conshohocken, PA: ASTM International.

Cheng, Q., Tang, C. S., Xu, D., Zeng, H., & Shi, B. (2021). Water Infiltration in a Cracked Soil considering Effect of Drying-wetting Cycles. Journal of Hydrology, 593.

Cossu, R., & Stegmann, R. (2018). Waste Management Strategies and Role of Landfilling. In R. Cossu, R. Stegmann (Eds.), Solid Waste Landfilling, Chapter 2.1, Elsevier, (pp.)3-13. https://doi.org/10.1016/B978-0-12-407721-8.00001-2

Day, R. W. (1994). Swell-shrink behaviour of compacted clay. Journal of Geotechnical Engineering, ASCE, 120(3): 618- 623.

Devapriya, A. S., & Thyagaraj, T. (2021). Swell-shrink and hydraulic behaviour of compacted red soil-bentonite mixture IOP Conference Series: Earth and Environmental Science, 727 012011

Julina, M., & Thyagaraj, T. (2021). Effect of hydraulic gradient on swell and hydraulic response of desiccated expansive soil – an experimental study. International Journal of Geotechnical Engineering, 16(2): 143-157.

Li, J. H., Li, L., Chena, R., and Li, D. Q. (2016). Cracking and vertical preferential flow through landfill clay liners. Engineering Geology, 206, 33-41.

McBrayer, M. C., Mauldon, M., Drumm, E. C., & Wilson, G. V. (1997). Infiltration tests on fractured compacted clay. Journal of Geotechnical and Geoenvironmental Engineering, 123(5), 469-473.

Ranjan, R. S., & Karthigesu, T. (1996). A capillary flow meter for measuring the hydraulic conductivity of clay under low gradients. Canadian Geotechnical Journal, 33 (3): 504–509.

Thyagaraj, T., & Zodinsanga, S. (2014). Swell-shrink behaviour of lime precipitation treated soil. Ground Improvement, Institution of Civil Engineers 167 (4): 260–273.